https://doi.org/10.37434/tpwj2021.02.04

# INFLUENCE OF HEAT TREATMENT ON THE PROPERTIES OF WELDED JOINTS OF V1341 ALLOY UNDER MODELED OPERATING CONDITIONS

**L.I. Nyrkova, T.M. Labur, S.O. Osadchuk, M.R. Yavorska** and **V.A. Koval**
E.O. Paton Electric Welding Institute of the NAS of Ukraine
11 Kazymyr Malevych Str., 03150, Kyiv, Ukraine. E-mail: office@paton.kiev.ua

The paper presents the results of comparative studies of corrosion-mechanical resistance of welded joints of V1341 alloy 1.2 mm thick, produced by manual argon-arc welding with free and constricted arc, after different types of heat treatment (HT) — artificial aging and complete cycle heat treatment (hardening and artificial aging). It was shown that artificial aging increases the strength characteristics of welded joints: those produced by free arc — by ~23 %, compared to the base metal, by constricted arc — by ~29 %, but reduces the relative elongation by ~82 % and ~84 %, and the strength coefficient — to 0.77 and 0.71 (0.81 and 0.83 in as-welded state), respectively. The complete cycle of HT provides increase in both strength and ductility. After artificial aging, as well as after a complete heat treatment cycle, the potential difference between the base metal and the HAZ does not exceed the permissible value of 0.05 V (according to GOST 9.005), which will not be dangerous at operation in nonaggressive environments. Artificial aging and full HT cycle do not impair the resistance of welded joints of V1341T alloy to exfoliating corrosion compared to as-welded state, which is assessed as value 2. An increase of resistance to intercrystalline corrosion (ICC) after artificial aging was demonstrated, the maximum depth of which was 0.301 mm for a joint produced by a free arc, and 0.233 mm — for a joint produced by a constricted arc (in as-welded state it was 0.350 mm and 0.47 mm, respectively). After a complete HT cycle, the ICC depth was 0.287 mm and 0.345 mm, respectively. Artificial aging reduces the corrosion-mechanical resistance of welded joints produced by free and constricted arc: the time-to-fracture of the samples was 9 and 12 days, respectively (compared to 45 days in as-welded state), but after a cycle of HT maximum time-to-fracture of welded joints increased to 54 and 31 days, respectively. Welded joints produced by a constricted arc had higher corrosion-mechanical resistance after a complete heat treatment cycle. 14 Ref., 5 Tables, 7 Figures.

*Keywords: aluminium alloy, welded joints produced by free and constricted arc welding, mechanical properties, structure, intercrystalline corrosion, exfoliating corrosion, corrosion under constant strain, potentiometry, voltamperometry*

Aluminium alloys of Al–Mg–Si–Cu alloying system combine a wide range of properties: high adaptability-to-fabrication, strength, weldability and corrosion resistance [1, 2]. Sheet alloy V1341 from this group is widely used to manufacture cylinders of different designs for storage of liquid substances [3]. During manufacture of such tanks their individual elements are joined by nonconsumable electrode manual argon-arc welding by a free or constricted arc [1, 2, 4]. However, the process of welding by a free arc takes place at its low penetrability in weld formation [2]. Application of constricted arc welding improves the weld shape and promotes lower softening of the joint after welding [1]. As the thermal cycle of nonconsumable electrode welding leads to welded joint softening, the items are heat treated before operation.

A lot of investigations are devoted to the influence of heat treatment operations on the change of properties of aluminium alloys, but they predominantly study the base metal behaviour [5, 6]. As the state of as-welded metal is unique for each thickness of the semi-finished product by material structure, and there is not enough such data in publications, the objective of this work was establishing the impact of different heat treatment modes on the set of service properties of the welded joints of sheet aluminium alloy V1341T (δ = 1.2 mm), produced by argon-arc welding by a free and constricted arc.

This paper is a continuation of a series of experimental studies, the results of which are presented in works [7–10].

**Experimental procedure**. Investigations were conducted on welded joints of aluminium alloy of V1341 grade of the following chemical composition (spectral analysis was performed in DFS-36 spectrometer), wt.%: Al — base, (0.45–0.9) Mg, (0.5–1.2) Si, (0.15–0.35) Mn, (0.1-0.5) Cu, (0.05–0.1) Ca, 0.25 Cr, 0.2 Zn, 0.15 Ti, 0.5 Fe, and not more than 0.1 of other

L.I. Nyrkova — https://orcid.org/0000-0003-3917-9063, T.M. Labur — https://orcid.org/0000-0002-4064-2644,
S.O. Osadchuk — https://orcid.org/0000-0001-9559-0151, M.R. Yavorska — https://orcid.org/0000-0003-2016-6289,
V.A. Koval — https://orcid.org/0000-0001-5154-1446

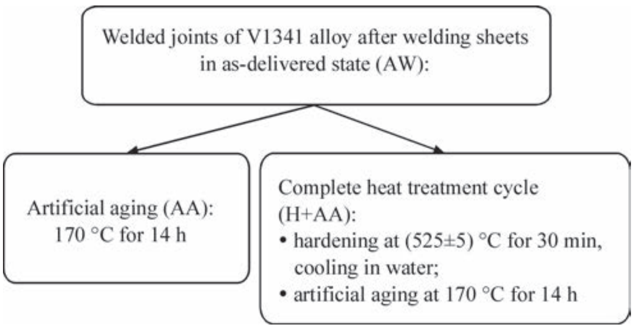


**Figure 1.** Scheme of conducting studies of V1341T alloy joint and applied modes of their heat treatment

elements. Wire of Sv2117 grade of 2 mm diameter was used for welding the alloy. Technological aspects of welding were discussed in detail in previous works [7–9]. In this work, joints welded along the rolling direction were investigated. The schematic of studying the joints and applied modes of their heat treatment are presented in Figure 1.

Features of structural transformations in welded joints produced with a free and constricted arc, were studied on metallographic sections, cut out normal to the weld axis. Sections were prepared by a standard procedure, and the microstructure was revealed by electrolytic etching in a solution of the following composition: 930 ml $CH_3COOH$ + 70 ml $HClO_4$.

Electrochemical studies were conducted in a solution of 3 % NaCl by potentiometry and voltamperometry methods with application of PI-50-1.1 potentiostat and Pr-8 programmer. The nature of potential distribution over the welded joint surface was studied by the method of measuring the potential under the drop by PWI procedure. Pressure electrochemical cell was used to obtain polarization curves. The working electrodes were individual zones of the welded joint, the reference electrode was saturated chloride-silver electrode EVL-1M1, and additional electrode was platinum. Potential sweep rate in potentiodynamic mode was $5\cdot10^{-4}$ V/s. Before taking the polarization curves, the sample surface was prepared by a standard procedure.

Resistance to intercrystalline corrosion (ICC), exfoliating corrosion and corrosion cracking was assessed in keeping with the requirements of GOST 9.021 [11], GOST 9.904 [12], and GOST 9.019 [13]. Testing for corrosion cracking was conducted under the condition of continuous axial tensile stress in the metal on the level of 160 MPa at full immersion of welded joint samples into the solution of 3 % NaCl in «Signal» unit for not less than 45 days. The weld was located normal to the direction of tensile stress action.

**Results and discussion**. *Macro- and microstructure of welded joints.* Figures 2 and 3 show the macro- and microstructure of base metal of V1341T alloy and its welded joints, produced depending on the welding process and kind of applied heat treatment. The weld form factor of the joint produced by a constricted arc is approximately 4 % higher, compared to the welded joint, produced with a free arc (2.52 and 2.43, respectively) [9].

Analysis of the microstructure of welded joints of V1341T alloy in naturally aged condition revealed that under the conditions of action of the thermal cycle of welding, decomposition of oversaturated solid solution and dissolution of the strengthening phases take place, irrespective of the kind of the arc. Solidification of molten weld metal at cooling is accompanied by precipitation of secondary phases and coagulation of insoluble phases (Figure 3, *a*). It is due to a considerable number of the main alloying elements and additives in the alloy composition [3]. In keeping with the constitutional diagram of Al–Mg–Si–Cu–Fe system, the following binary phases can be in equilibrium with the solid solution in the alloy: $Mg_2Si$, $SiCuAl_2$, $FeAl_3$, $Mg_5Al_8$, as well as ternary phase: $CuFeAl_5$, $CuMgAl_2$, $FeSiAl_2$, $FeMg_3Si_6$. During weld solidification they form the same quanti-

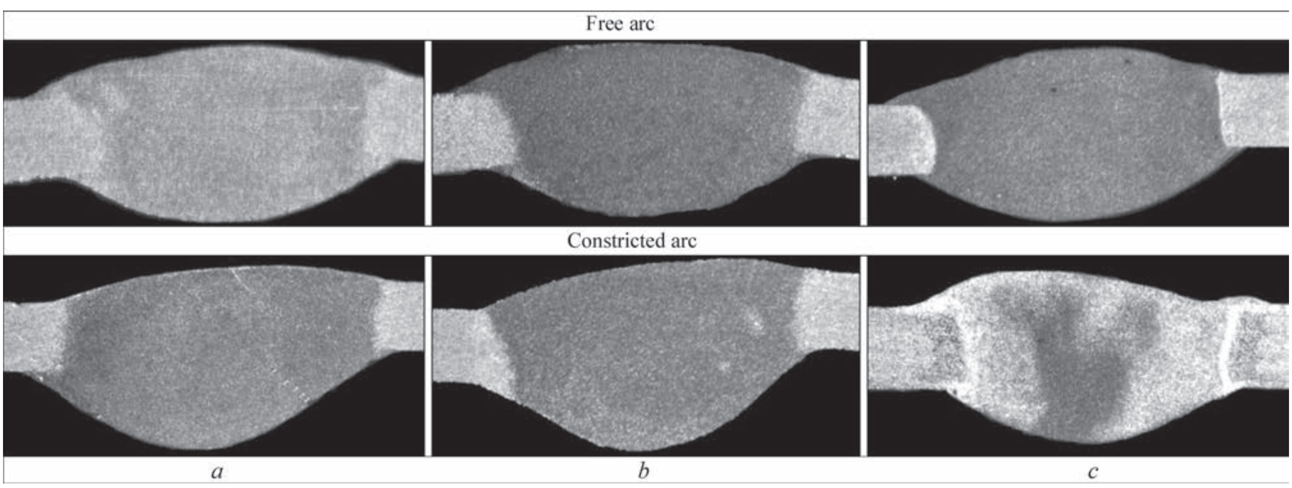


**Figure 2.** Macrosections of welded joints of V1341 alloy, produced by free and constricted arc, in different states: *a* — in as-welded state; *b* — after artificial aging; *c* — after a complete heat treatment cycle

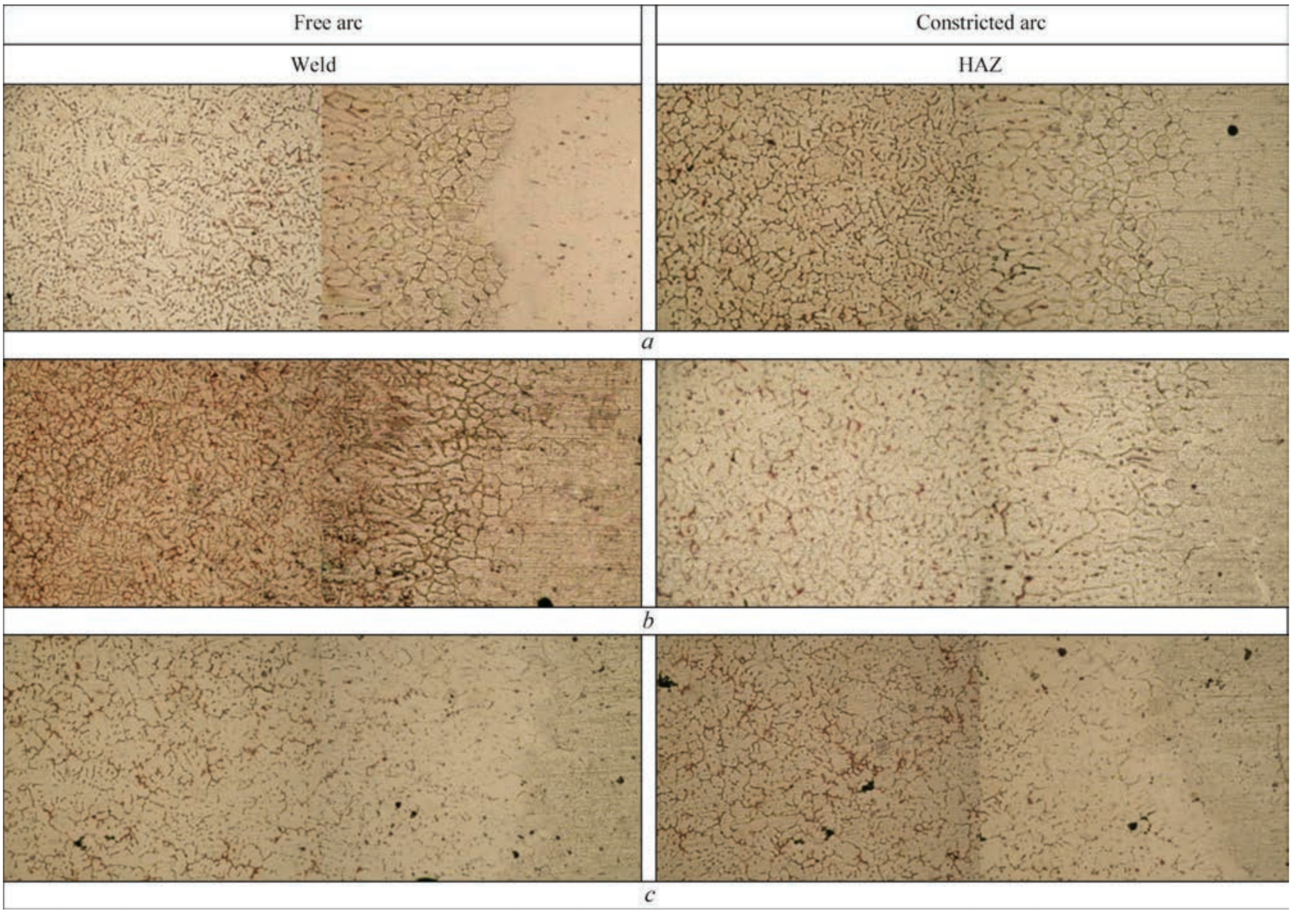


**Figure 3.** Microstructure (×320) of welded joints of V1341T alloy produced by constricted and free arc, in different states: *a* — as-welded state; *b* — after artificial aging; *c* — after a complete heat treatment cycle

ty of metastable phases, which are uniformly located, but differ by their shape and geometrical dimensions. Their characteristic feature is instability of decomposition within one grain [3]. Boundary areas of the crystallites are enriched in alloying elements, and their bulk is depleted in them, while thin eutectic interlayers form along the boundaries.

Microstructure of the zone of weld fusion with the base metal has melted-off grain boundaries, which formed under the action of heating at welding. Contact melting of the grains between each other or with eutectic phase $Mg_2Si$, which is located along the grain boundaries, results in their thickening. Fast removal of the arc, metal solidification and weld formation lead to formation of columnar crystals, oriented normal to the direction of the vector of arc movement, near the fusion boundary of the weld and base metal (Figure 3, *b*). From the base metal side, decomposition of oversaturated solid solution and simultaneous dissolution of earlier formed strengthening phases and precipitation of secondary phases proceed in the fusion zone. Coagulation of insoluble intermetallic phases of iron and silicon, which penetrate into the metal at the stage of metallurgical production of the alloy, and can cause higher stresses in the structure, also takes place [1].

In the HAZ area of V1341T alloy joints an increase of grain size and coagulation of insoluble phase inclusions, and complete or partial lowering of the strengthening effect after natural aging are observed, as well as local annealing and hardening of individual structural component areas (Figure 3, *c*). Interaction of boundary inclusions of intermetallics with the solid solution here causes formation of areas with liquid interlayers of low-melting eutectics along the grain boundaries. This is due to the features of structural and phase transformations in the metal under the impact of the thermal cycle of arc welding.

Performance of the operation of artificial aging of the joint samples leads to an increase of volume fraction of secondary phases and their density in the weld structure (Figure 3, *a, b*). The process is accompanied by thickening of grain boundaries as a result of their contact fusion with each other or with $Me_2Si$ eutectic phase located near the grain boundaries. The above-mentioned microstructural transformations proceed as a result of solid solution decomposition, and strain hardening of phases that improves the strength of welded joint metal (Table 1).

Performance of a complete cycle of heat treatment of the joints (hardening and artificial aging) leads to a

**Table 1.** Mechanical properties of base metal and welded joints of V1341T alloy produced by free and constricted arc, after heat treatment by different modes

| Sample state | $\sigma_t$, MPa | $\sigma_{0.2}$, MPa | δ, % | α, deg | WJ strength coefficient | $\sigma_t$, MPa | $\sigma_{0.2}$, MPa | δ, % | α, deg | WJ strength coefficient |
|---|---|---|---|---|---|---|---|---|---|---|
| | Welded joint produced by a free arc | | | | | Welded joint produced by constricted arc | | | | |
| As-welded (AW) | 195.0 / 250.5 | 130.11 / 87.6 | 2.6 / 18.9 | 56 / 180 | 0.83 | 200.32 / 50.5 | 144.31 / 87.6 | 1.7 / 18.9 | 66 / 180 | 0.81 |
| After artificial aging (AA) | 257.63 / 35.7 | 215.53 / 13.3 | 1.9 / 10.7 | 30 / 180 | 0.76 | 258.73 / 35.7 | 204.03 / 13.3 | 1.7 / 10.7 | 46 / 180 | 0.77 |
| After hardening and artificial aging (H + AA) | 241.53 / 21.1 | 288.6 / 282.0 | 6.9 / 10.7 | 35 / 158 | 0.75 | 323.03 / 21.1 | 294.32 / 82.0 | 3.3 / 10.7 | 43 / 158 | 1.00 |

*Note*. Values of welded joint properties in the respective state are given in the numerator, those of base metal —– in the denominator.

change of grain dimensions, width of interlayers between them and to presence of secondary phase inclusions in the structure, etc (Figure 3, *a*). Precipitation of additional secondary phase inclusions and uniform nature of their distribution over the entire weld volume has a positive impact on mechanical properties of welded joints (Table 1). On the boundary of weld fusion with base metal, formation of thinner boundaries of structural components is noted (Figure 3, *c*). They are associated with presence of small copper additives (0.3 %) in the alloy that by the data of work [3] limits the rate of precipitation of Guinier–Preston zones which are in a metastable equilibrium with the solid solution. The morphology of phase precipitates from the matrix is of a homogeneous nature, and phase dimensions are dispersed. It is determined by quick fixation of structural components at hardening of joint samples in water. Performance of artificial aging operation after hardening allows preserving the morphology of structural component location, as well as shape and dispersed dimensions of phase inclusions. Thickening of the boundaries of weld crystallites and base metal grains is noted in individual areas in the zone of fusion with the base metal. Their total thickness is smaller than in the structure of welded joints after artificial aging (Figure 3).

As was noted above, structural transformations, occurring in V1341T alloy during welding with a free and constricted arc and further heat treatment of the welded joints, influence their mechanical property values (Table 1). In keeping with the obtained data, the strength of joints welded by a free or constricted arc is equal to 195.0 and 200.3 MPa that is 22 and 20 % lower than base metal strength. Strength coefficients of the joints are equal to 0.83 and 0.81, respectively. The yield limit of welded samples, compared with base metal also decreases by 30 and 23 %, respectively (Table 1). Note that welding technology has a stronger impact on the level of ductility values, namely: relative elongation and bend angle decrease by 86 and 91 %, and by 70 and 63 %, respectively.

After artificial aging, the welded joint strength characteristics become higher compared to as-welded conditions. At application of a free arc, strength is equal to 257.6 MPa that is by ~23 % lower than that of base metal in the same condition, and with a constricted arc it is 258.7 MPa (by ~ 29 % lower). At the same time, lowering of the strength coefficient to the level of 0.76 and 0.77 is observed. Yield limit also rises, however, its numerical values remain smaller compared with base metal: by 31 % for joints produced with a free arc, and by ~35 % for joints produced with a constricted arc (Table 1). Performance of artificial aging operation causes further lowering of the values of ductility (bend angle and relative elongation), by ~83 and ~82 % for a joint produced with a free arc, and by ~74 and ~84 % for a joint produced with a constricted arc (Table 1), respectively.

Performance of the operation of complete heat treatment cycle causes a 25 % increase of strength in joints produced with a free arc (up to 241.5 MPa), compared to base metal. In joints, produced by a constricted arc, strength increased up to 323.0 MPa almost to base metal level (321.1 MPa). The value of strength coefficient of the joints was equal to 0.75 and 1.0 %, respectively. Positive impact of the heat treatment mode was observed in the values of yield limit, which rose and even somewhat exceeded the base metal level and was equal to 288.6 and 294.3 MPa for joints produced by a free and constricted arc. An increase of the level of relative elongation of the joints up to 6.9 to 3.3 % was also observed (Table 1). At the same time, the level of bend angle was smaller, compared to as-welded state and almost the same, compared to samples after artificial aging: 35 % (for a free arc) and 43 % (for a constricted arc).

Thus, after a complete heat treatment cycle an increase of strength characteristics to base metal level, was found in samples of welded joints produced by a

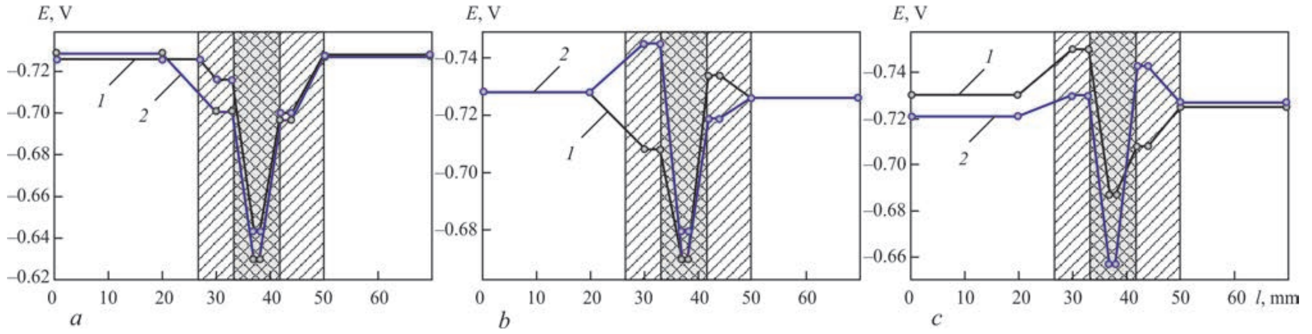


**Figure 4.** Nature of distribution of electrochemical potentials under the drop in different zones of welded joints of V1341T alloy, produced by a free (*1*) and a constricted (*2*) arc, as well as in different states: *a* — after welding; *b* — after artificial aging; *c* — after complete heat treatment cycle

**Table 2.** Difference of potentials between the zones of V1341T alloy welded joint in different states

| Difference of potentials between welded joint zones, V | Welded joint state | | | | | |
|---|---|---|---|---|---|---|
| | Free arc | | | Constricted arc | | |
| | AW | AA | H+AA | AW | AA | H+AA |
| Base metal — weld | 0.099 | 0.042 | 0.041 | 0.117 | 0.066 | 0.044 |
| Base metal — HAZ | 0.030 | 0.015 | 0.010 | 0.068 | 0.013 | 0.032 |

constricted arc that is, probably, due to reduction of electrochemical heterogeneity of the joint structure, as a result of formation of a fine-grained structure and narrowing of the HAZ under the impact of a more concentrated arc energy due to its compression by argon [1].

*Electrochemical studies*. Measurement of corrosion potentials in the studied samples showed that the difference of potentials between the base metal and weld for as-delivered welded joints is equal to ~0.099 V (free arc) and ~0.117 V (constricted arc) (Figure 4, Table 2). Both kinds of heat treatment applied after welding, reduce the above difference, which after artificial aging was equal to ~0.042 V (free arc) and ~0.066 V (constricted arc), and after a complete heat treatment cycle: ~0.041 V (free arc) and 0.044 V (constricted arc), respectively. The difference of potentials between the base metal and HAZ for as-delivered welded joints was smaller compared to the weld, and it was equal to ~0.030 V (free arc) and ~0.068 V (constricted arc). After heat treatment of the samples the difference of potentials between base metal and HAZ became even smaller, namely after artificial aging it was equal to ~0.015 V (free arc) and ~0.013 V (constricted arc), and after a complete heat treatment cycle it was ~0.010 V (free arc) and ~0.032 V (constricted arc), respectively.

Thus, the operations of sample heat treatment reduce the difference of potentials between base metal and HAZ to admissible values, except for joints, welded by a free arc after artificial aging. The difference of potentials between base metal and HAZ after both the applied kinds of heat treatment did not exceed the admissible level (0.05 V), in keeping with GOST 9.005 [14].

Polarization curves of base metal and weld in joints produced by a free and a constricted arc in different states are given in Figure 5. Their analysis showed

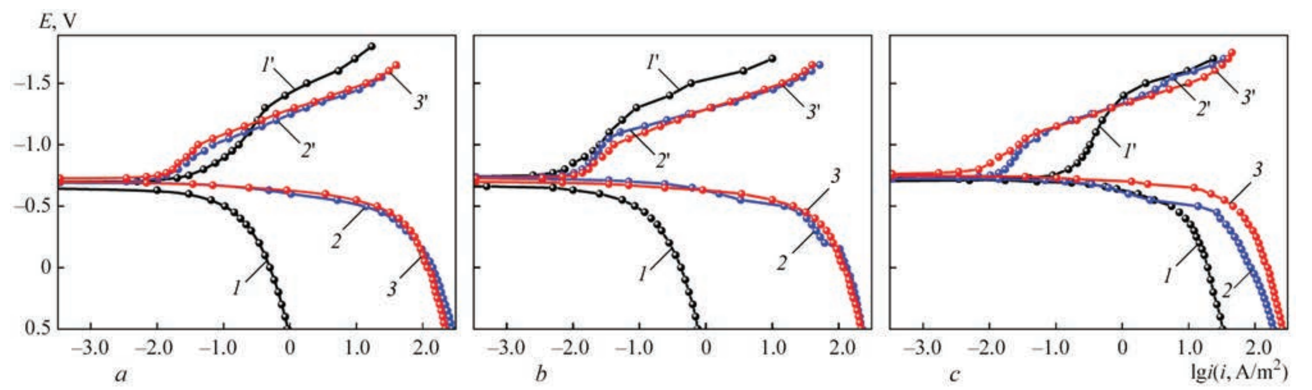


**Figure 5.** Anode (*1*, *2*, *3*) and cathode (*1*′, *2*′, *3*′) polarization curves of base metal (*1*, *1*′) and welded joints of V1341T alloy, produced by a free arc (*2*, *2*′) and constricted arc (*3*, *3*′) in different states: *a* — as-welded; *b* — after artificial aging; *c* — after hardening and artificial aging

**Table 3.** Electrochemical characteristics of base metal and weld of V1341T alloy joints produced by a free and a constricted arc in 3 % NaCl

| Sample characteristic | Sample state | $E_{cor}$, V | $i_a$, A/m$^2$ | $i_d$, A/m$^2$ | $E_{H_2}$, V |
|---|---|---|---|---|---|
| BM | As-delivered (natural aging) | –0.728 | 0.03 | 2.95 | –1.38 |
| | AA | –0.724 | 0.015 | 0.026 | –1.32 |
| | H+AA | –0.715 | 1.79 | 0.33 | –1.42 |
| WJ produced by a free arc | As-welded | –0.699 | 1.07 | 0.023 | –0.99 |
| | AA | –0.726 | 1.09 | 0.023 | –1.06 |
| | H+AA | –0.729 | 1.80 | 0.026 | –0.99 |
| WJ produced by a constricted arc | As-welded | –0.708 | 3.37 | 0.016 | –1.05 |
| | AA | –0.736 | 1.09 | 0.022 | –1.0 |
| | H+AA | –0.737 | 21.88 | 0.02 | –1.07 |

*Note*. $i_a$ — anode dissolution current at –0.6 V potential; $i_d$ — limit diffusion current; $E_{cor}$ — corrosion potential; $E_{H_2}$ — hydrogen evolution potential.

that the anode dissolution current (at –0.6 V potential) in the weld of samples of both the joints in as-welded condition (Figure 5, curves *2*, *3*) is higher than that in the base metal: 1.07 A/m$^2$ (free arc), 3.37 A/m$^2$ (constricted arc) and 0.03 A/m$^2$ — base metal (Table 3).

Heat treatment by artificial aging mode reduces the anode currents in the weld, which were 1.09, 1.09 and 0.015 A/m$^2$ (Table 3), respectively. After a complete heat treatment cycle, the difference between the anode dissolution current of base metal and the anode dissolution currents of the welds was equal to 1.79 A/m$^2$ for base metal, and 1.80 and 21.88 A/m$^2$ for joints produced by a free and constricted arc, respectively. Cathode curves for welds in as-welded state shift to the area of lower currents, compared with base metal (Figure 5, *a*). Limit diffusion current in welds of both the studied methods of joining V1341T alloy is smaller (0.023 and 0.016 A/m$^2$), than in base metal (2.95 A/m$^2$) that may point to inhibition of the cathode process in weld metal (Table 3).

After artificial aging a slight increase in boundary diffusion current is observed in the metal of welds of both the joints, compared to as-welded state (0.023 A/m$^2$ (free arc), 0.022 A/m$^2$ — constricted arc, 0.0263 A/m$^2$ — base metal) (Figure 5, *b*, curves *2*′, *3*′). It results in manifestation of the tendency to activation of the corrosion process in this area on the polarization curve. A complete cycle of joint heat treatment considerably inhibits the corrosion process in welds that is manifested in reduction of the values of limit diffusion current to 0.026 A/m$^2$ (free arc), and 0.0202 A/m$^2$ (constricted arc), compared with base metal (0.33 A/m$^2$) (Figure 5, *c*, curves *2*′, *3*′) (Table 3). It should be noted that no significant difference in weld metal behaviour was found in joints produced by a free and constricted arc. Since in aqueous media, as indicated by the shape of polarization curves, corrosion of V1341T alloy occurs with diffusion control, the corrosion rate can be evaluated by values of limit diffusion current [14].

Thus, it was determined that heat treatment of welded joints of V1341T alloy by artificial aging mode promotes a slight increase of corrosion rate, but at the same time, lowers the potential of hydrogen evolution from the HAZ metal with both the studied welding methods, compared to base metal. Performance of a complete heat treatment cycle reduces the limit diffusion current and potential of hydrogen evolution in welds, irrespective of the welding process, compared to base metal. One can expect that with such HT mode, the corrosion resistance of the alloy welded joint metal will increase.

*Intercrystalline corrosion resistance (ICC).* Maximum of depth of base metal ICC in as-delivered

**Table 4.** Generalized results of assessment of corrosion-mechanical resistance of welded joints of V1341T alloy, produced by different technologies of nonconsumable electrode welding

| Sample characteristic | Sample state | ICC depth, mm | Exfoliating corrosion resistance, num | Time-to-fracture, days |
|---|---|---|---|---|
| Base metal | As-delivered | 0.082–0.086 | 2–3 | 67–88 |
| | After artificial aging | 0.074–0.117 | | 47–77 |
| | After hardening and artificial aging | 0.111–0.209 | | 45–87 |
| WJ produced by base arc | As-welded | 0.245–0.350 | | 10–45 |
| | After artificial aging | 0.123–0.301 | | 3–9 |
| | After hardening and artificial aging | 0.214–0.287 | | 4–54 |
| WJ produced by constricted arc | As-welded | 0.289–0.467 | | 9– > 45 |
| | After artificial aging | 0.062–0.233 | | 9–12 |
| | After hardening and artificial aging | 0.074–0.345 | | 9–31 |

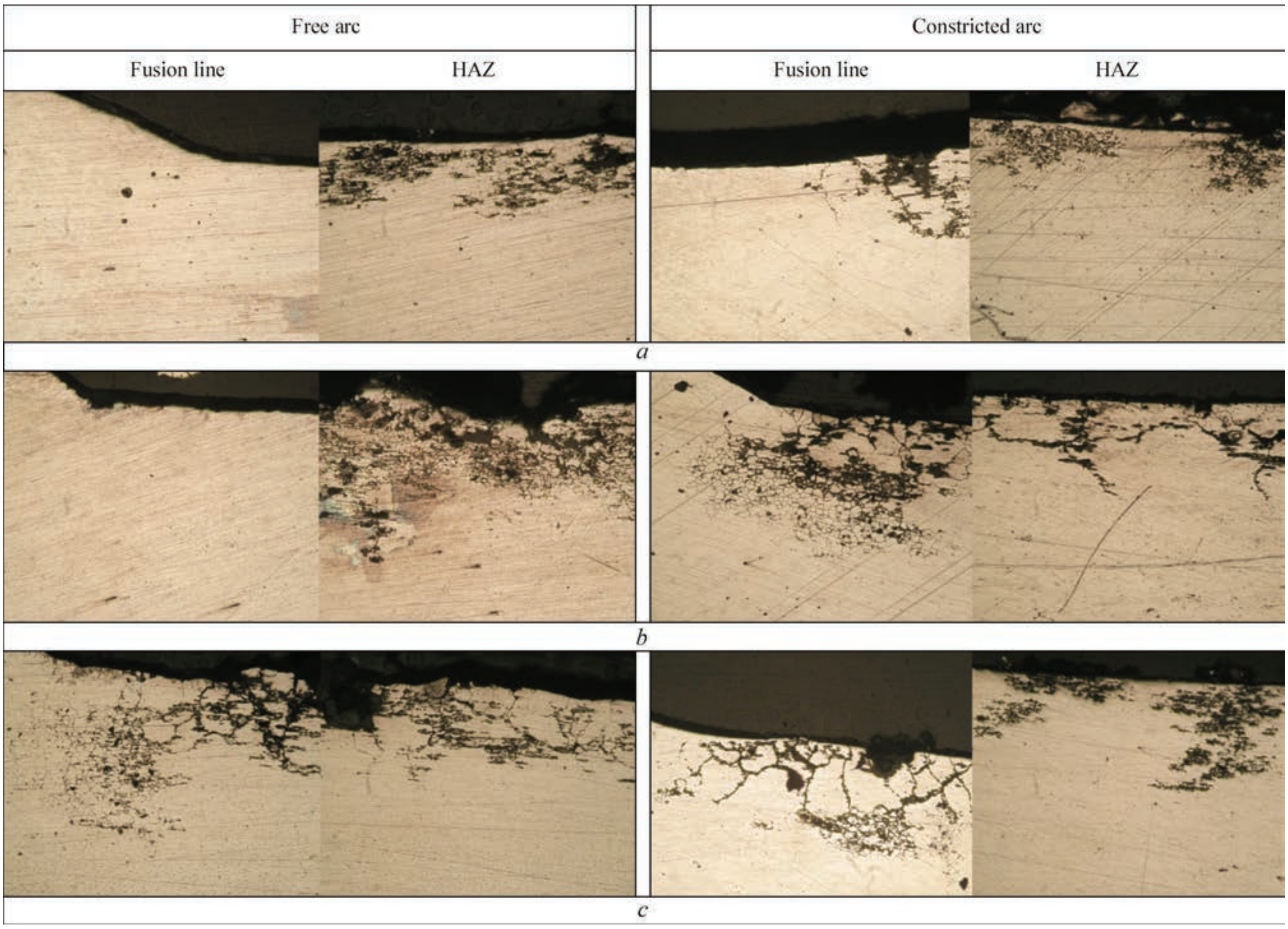


**Figure 6.** Appearance of samples in the fusion zone and HAZ of welded joints of V1341T alloy, produced by constricted and free arc, in different states, after testing for intercrystalline corrosion resistance, ×320: *a* — after welding; *b* — after artificial aging; *c* — after complete heat treatment cycle

condition is equal to approximately 0.086 mm. The intercrystalline fracture sites of welded joints produced with a free arc, were noted in the HAZ, and they developed to the depth of 0.350 mm (Table 4), and in those produced with a constricted arc they were found in the fusion zone and HAZ (Figure 6, *a*) to the depth of 0.506 mm. Artificial aging of joint samples caused a slight increase of metal sensitivity to ICC: intercrystalline cracks propagated in the HAZ of the joints produced by a free arc (Figure 6, *b*), to the maximum depth of 0.301 mm, and in the HAZ of joints produced by a constricted arc — to 0.233 mm. After a complete HT cycle intercrystalline cracks formed both in the HAZ and in the fusion zone of both the welded joints (Figure 6, *c*), ICC depth was 0.287 and 0.345 (0.533) mm, respectively (Table 5).

Thus, welding sheet alloy V1341 1.2 mm thick by a constricted arc causes a lowering of ICC resistance

**Table 5.** Results of assessment of exfoliating corrosion resistance of V1341T alloy welded joints produced by free and constricted arc in different states

| Sample characteristic | Index description | | | | | | | | Index value, number |
|---|---|---|---|---|---|---|---|---|---|
| | Nature of change in sample appearance | Largest delamination diameter, mm | Delamination area on each surface, % | | Total length of cracked end faces, mm | | | | |
| | | | A | B | 1 | 2 | 3 | 4 | |
| Welded joints produced by free arc | | | | | | | | | |
| AW | Delamination | <1.0 | <1.0 | <1.0 | 0 | 0 | 0 | 0 | 2–3 |
| AA | Surface darkening | 0 | 0 | 0 | 0 | 0 | 0 | 0 | 2 |
| H+AA | Surface darkening | 0 | 0 | 0 | 0 | 0 | 0 | 0 | 2 |
| Welded joints produced by constricted arc | | | | | | | | | |
| AW | No changes | 0 | 0 | 0 | 0 | 0 | 0 | 0 | 1 |
| AA | Surface darkening | 0 | 0 | 0 | 0 | 0 | 0 | 0 | 2 |
| H+AA | Surface darkening | 0 | 0 | 0 | 0 | 0 | 0 | 0 | 2 |

of welded joints, but well-chosen heat treatment mode can ensure increase of their intercrystalline fracture resistance.

*Exfoliating corrosion resistance.* Analysis of the surface of samples of welded joints produced by free arc (in as-welded condition) revealed delamination centers of almost 1 mm diameter, of the total area of not more than 1 %. No other indices reflecting a change in the appearance of studied sample surface were revealed (Table 5). Surface darkening was the main characteristic indication of a change in the properties of the joints after artificial aging or complete heat treatment cycle. Exfoliating corrosion resistance was evaluated by number 2. In welded joints produced by constricted arc, the value of exfoliating corrosion resistance in as-welded state was assessed by number 1, as no changes on the sample surface or end faces were found. After artificial aging or a complete cycle of joint heat treatment, a change of the sample surface colour was observed. Their exfoliating corrosion resistance was also assessed by number 2 to GOST 9.904. Thus, the surface colour change was found to be the only characteristic indicating a change in the properties of samples of both the kinds of welded joints after heat treatment, and exfoliating corrosion resistance was assessed as number 2.

*Corrosion cracking resistance.* Appearance of samples after testing for resistance to corrosion-mechanical cracking is shown in Figure 7. As revealed by visual analysis of the samples after welding and artificial aging, they failed in the base metal in the HAZ at 4–5 mm distance, and after conducting complete heat treatment of the samples — near the fusion zone with base metal. The time-to-fracture of welded samples produced by free arc decreased to 10–45 days (20 days on average), compared to base metal, for which it was from 67 to 88 days (almost 73 days) (Table 4).

Similar results were obtained for joints, welded by constricted arc. After artificial aging, the period of time to complete destruction of the samples was the shortest for both the studied methods of joining V1341T alloy. For joints produced by free arc, fracture occurred within 3–9 days, and for those produced by constricted arc it was 9–12 days. After a complete heat treatment cycle the maximum time-to-fracture of base metal was 87 days, of welded joints — 54 and 31 days, respectively.

Thus, heat treatment by the mode of hardening and artificial aging increases the corrosion-mechanical resistance of welded joints, both those produced by free and constricted arc. At the same time, mechanical property values after performance of a complete heat treatment are higher for joints, produced by a constricted arc. The highest level of corrosion-mechanical resistance as a result of conducting a complete heat treatment cycle is achieved in samples of welded joints produced by constricted arc.

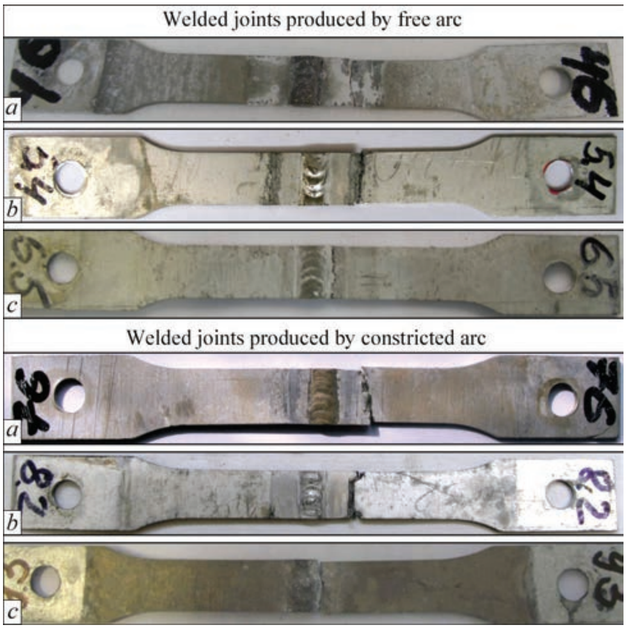


**Figure 7.** Appearance of samples of V1341T alloy welded joints produced by free and constricted arc, after testing for corrosion cracking resistance: *a* — as-welded state; *b* — after artificial aging; *c* — after complete heat treatment cycle

## Conclusions

1. Conducting the artificial aging operation improves the strength properties of welded joints produced by free arc up to 257.6 MPa (by ~23 %, compared to base metal), by constricted arc — up to 258.7 MPa (by ~29 %). However, a lowering of the coefficient of strength of the joints to 0.76 and to 0.77 (0.81 and 0.83 in as-welded condition) is noted here. The value of relative elongation of the samples decreases by ~82 % for joints produced by free arc, and by ~84 % for joints produced by constricted arc. Performance of a complete heat treatment cycle ensures an increase of both strength and ductility values. The values of ultimate strength of the joints produced by free arc, rose by ~25 %, compared to base metal, and those of joints produced by constricted arc, increased to base metal level. The coefficients of strength of the joints were equal to 0.75 and 1.0, respectively. Relative elongation value also rose to the level of 6.9 and 3.3 %, respectively.

2. By the results of electrochemical investigations, it was determined that after heat treatment, both by the artificial aging mode, and after a complete cycle of heat treatment, the difference of potentials between base metal and HAZ did not exceed the admissible value (0.05 V), in keeping with GOST 9.005 that is not dangerous under the conditions of operation of V1341T alloy products in nonaggressive media.

3. Heat treatment by artificial aging mode promotes a slight increase of limit diffusion current (corrosion rate) of welded joints produced by free and constricted arc, but at the same time, it reduces the hydrogen evolution potential in welds of these joints, compared to base metal. A complete heat treatment cycle reduces the limit diffusion current and potential of hydrogen evolution in welds, produced by both the technologies of joining V1341T alloy that is indicative of an increase of corrosion resistance of welds.

4. It is found that conducting artificial aging or a complete heat treatment cycle of welded joints of V1341T alloy produced by a free or constricted arc, does not impair their exfoliating corrosion resistance, assessed by number 2.

5. Performance of artificial aging improves the intercrystalline corrosion resistance of V1341T alloy and its joints: cracks develop in the HAZ of the joint, produced by a free arc, to the maximum depth of 0.301 mm, and in the joint made by a constricted arc — to 0.233 mm (in as-welded state — 0.350 and 0.47 mm, respectively). After performance of a complete HT cycle, the depth of intercrystalline cracks is equal to 0.287 and 0.345 (0.533) mm, respectively.

6. Heat treatment by the artificial aging mode lowers the corrosion-mechanical resistance of welded joints produced by a free or constricted arc: time-to-fracture of the samples is reduced to 9 and 12 days, respectively (compared to as-welded state — 45 days). After a complete heat treatment cycle the maximum time-to-fracture of welded joints rises to 54 and 31 days, respectively. Higher corrosion-mechanical resistance after the complete heat treatment cycle was demonstrated by samples of welded joints, produced by a constricted arc.

*The work was performed with the support of the NAS of Ukraine within the PWI departamental order program in 2017–2021 (State registration number 0117U001188).*

1. Ishchenko, A.Ya., Labur, T.M. (2012) *Welding of modern structures of aluminium alloys.* Kyiv, Naukova Dumka [in Russian].
2. Krivov, G.A., Ryabov, V.R., Ishchenko, A.Ya. et al. (1998) *Welding in aircraft construction.* MIIVTs [in Russian].
3. Ovchinnikov, V.V., Grushko, O.E. (2005) High performance welded aluminium alloy V1341 of Al–Mg–Si system. *Mashinostroenie i Inzhen. Obrazovanie*, 3(**4**), 2–11 [in Russian].
4. Albert, D. (1993) Aluminium alloys in arc welded constructions. *Welding World Magazine*, 32(**3**), 97–114.
5. Pogatscher, S., Antrekowitsch, H., Leitner, H. et al. (2013) Influence of the thermal route on the peak-aged microstructures in an Al–Mg–Si aluminium alloy. *Scripta Mater*., **68**, 158–161.
6. Fridlyander, I.N., Grushko, O.E., Shamraj, V.F., Klochkov, G.G. (2007) High-strength structural alloy Al–Cu–Li–Mg of lower density doped with silver. *Metallovedenie i Termich. Obrab. Metallov*, **6**, 3–7 [in Russian].
7. Koval, V.A., Labur, T.M., Yavorska, T.R. (2020) Properties of joints of V1341T grade alloy under the conditions of TIG welding. *The Paton Welding J.*, **2**, 35–40.
8. Nyrkova, L.I., Labur, T.M., Osadchuk, S.O., Yavorska, T.R. (2020) Corrosion and mechanical resistance of welded joints of aluminium B1341 alloy, produced by argon arc welding using free and constricted arc. *Ibid*., **12**, 40–47.
9. Nyrkova, L.I., Osadchuk, S.O., Kovalenko, S.Yu. et al. (2020) Influence of heat treatment on corrosion resistance of welded joint of aluminium alloy of Al–Mg–Si–Cu system. *Fizyko-Khimich. Mekhanika Materialiv*, **5**, 131–138 [in Ukrainian].
10. GOST 9.021–74: *Unified system of corrosion and ageing protection. Aluminium and aluminium alloys. Accelerated test methods for intercrystalline corrosion.* Moscow, Izd-vo Standartov [in Russian].
11. GOST 9.904–83: *Unified system of corrosion and ageing protection. Aluminium and aluminium alloys. Accelerated test methods for exfoliation corrosion.* Moscow, Izd-vo Standartov [in Russian].
12. GOST 9.019–74: *Unified system of corrosion and ageing protection. Aluminium and magnesium alloys. Accelerated test methods for corrosion cracking.* Moscow, Izd-vo Standartov [in Russian].
13. GOST 9.005–72: *Unified system of corrosion and ageing protection. Metals, alloys, metallic and non-metallic coatings. Permissible and impermissible contacts with metals and non-metals.* Moscow, Izd-vo Standartov [in Russian].
14. Zhuk, N.P. (1976) *Course of theory of corrosion and protection of metals.* Moscow, Metallurgiya [in Russian].

Received 18.01.2021